Journal of Alloys and Compounds 516 (2012) 5–8

Contents lists available at SciVerse ScienceDirect

Journal of Alloys and Compounds

journal homepage: www.elsevier.com/locate/jallcom

Letter

Study of the "All-Round-Effect" generated by aging in traction in a Ni rich TiNi shape memory alloy

R. Amireche [a], M. Morin [b,c], S. Belkahla [a,*]

[a] Laboratoire LEAM, Université Badji Mokhtar, BP 12, 23000, Annaba, Algeria
[b] Université de Lyon, CNRS, France
[c] INSA-Lyon, MATEIS UMR5510, F-69621 Villeurbanne, France

ARTICLE INFO

Article history:
Received 13 October 2011
Received in revised form
27 November 2011
Accepted 30 November 2011
Available online 13 December 2011

Keywords:
Shape memory alloys
All Round Effect
TiNi
Ti_3Ni_4

ABSTRACT

Following aging under stress, Ni-rich TiNi shape memory alloys are subject to a two-way shape memory effect known as the "All Round Memory Effect" (ARME). The latter causes a sample to return to its high temperature shape during heating after being spontaneously deformed on cooling during martensitic and *R*-phase transformations. This effect has been thoroughly studied for stresses in bending. In this work, we were able to generate ARME with tensile stresses, making it possible to make more quantitative measurements of the effect. Application of a static stress opposite spontaneous deformation during cooling also allowed quantifying the magnitude of internal stresses caused by Ti_3Ni_4 coherent precipitates during aging.

1. Introduction

TiNi shape memory materials are widely used at present [1–3]. In addition to their outstanding properties (shape memory effect, two-way shape memory effect, super-elastic effect), a specific characteristics of these alloys is their curious behavior known as the All Round Memory Effect (ARME). This effect is a special case of the two-way memory effect. The alloy spontaneously forms two different shapes during the thermal cycle between high and low temperatures. Nishida and Honma [4,5] were the first to highlight this fact by applying it to aging treatment under bending stress at moderate temperatures. They deduced the following from their works:

- ARME occurs only in Ni-rich TiNi alloys (at.%Ni $\geq$ 50.6).
- ARME is caused by the precipitation of coherent Ti_3Ni_4 particles. These precipitates produce stress fields strong enough to control the growth of *R* and martensitic phases.
- The range of aging temperatures allowing the emergence of ARME is from 670 K to 770 K.

The works of Sato et al. [6] and Gyobu et al. [7], which focused on Ni-rich TiNi films, have highlighted the influence of different aging parameters (time, temperature, strain) on ARME generated by aging under bending.

Most experiments on ARME have been performed by applying bending stress during heat treatment. In this paper we present results obtained by imposing tensile stress, in order to obtain more quantitative results.

2. Experimental procedure

The samples were cut from thin sheets of Ti-Ni in the form of ribbons with dimensions (0.1 mm × 3 mm × 10 mm). The composition of the alloy used is: Ti–51.8 at.% Ni. All the samples were subjected to homogenization treatment for 30 min at 923 K, followed by water quenching

Preliminary experiments allowed us to determine that, for the alloy studied, the maximum amplitude of ARME was obtained after aging for 24 h at 673 K. All the ARME results presented here were therefore obtained by using this method of heat treatment.

Thus ARME treatment consisted of 24 h annealing at 673 K under different static stresses (σ_{aging} = 0, 45, 95, 200, 300 and 400 MPa) by using an assembly designed specifically for this work (Fig. 1a).

The transformation temperatures were determined by using two techniques:

- Changes in measurements of electrical resistivity as a function of temperature (303–373 K).
- Differential Scanning Calorimetry (DSC) during thermal cycling from 173 to 373 K.

The thermomechanical behavior of the samples was characterized by a special tensile test machine for σ_{test} stress ranging from 0 to 150 MPa (Fig. 1b). The machine

* Corresponding author. Tel.: +213 07 73 87 86 73; fax: +213 0 38 87 53 97.
E-mail addresses: ar_phy@yahoo.fr (R. Amireche), michel.morin@insa-lyon.fr (M. Morin), soliman_belkahla@yahoo.fr (S. Belkahla).

0925-8388/$ – see front matter © 2011 Elsevier B.V. All rights reserved.
doi:10.1016/j.jallcom.2011.11.154

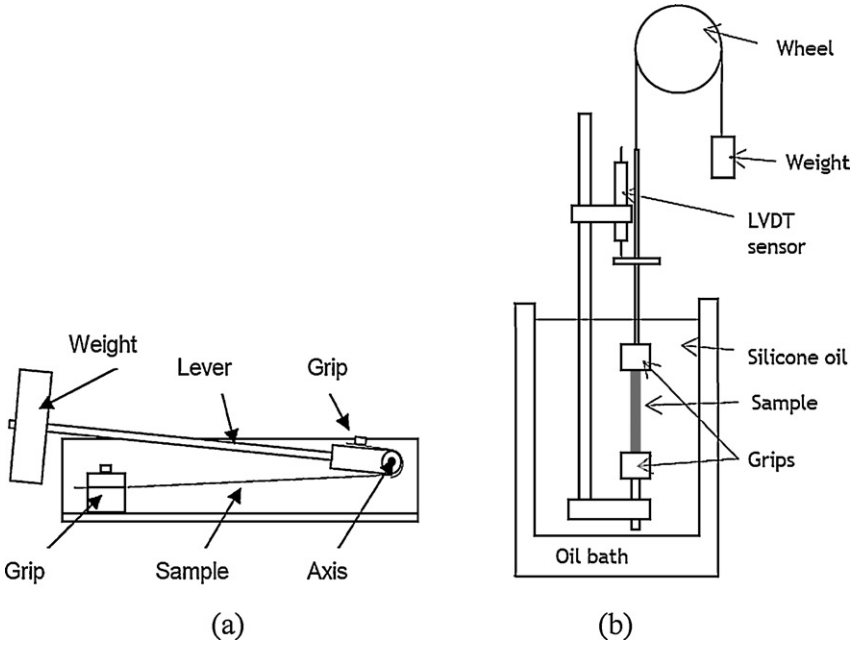

Fig. 1. Apparatus used for annealing under stress (a) and tensile machine (b).

used enabled simultaneous acquisition of the variation of deformation and electrical resistance of the sample under constant stress σ_{test} versus temperature between 230 and 400 K.

3. Results and discussion

3.1. Martensitic transformation in nickel rich TiNi alloy

DSC thermograms and resistivity curves with and without annealing are compared in Fig. 2. In Fig. 2a, the Ni-rich TiNi alloy, homogenized for 30 min at 923 K, presents a classical martensitic transformation in one step. The DSC thermogram shows a single peak on cooling at 243 K (M^*), indicating direct transformation ($A \rightarrow M$). On heating, reverse transformation ($M \rightarrow A$) is also characterized by a single peak at 270 K (A^*). Thermal hysteresis is about 30 K and transformation enthalpies ΔH are close to 15 J/g. After annealing for 24 h at 673 K (Fig. 2b), a second peak appears on cooling at 315 K (denoted R^*). This peak is characteristic of the R transformation $A \rightarrow R$, with a transformation enthalpy $\Delta H_{A \rightarrow R} = 6.3$ J/g. The same thermograms were obtained for samples aged with and without stress 24 h at 673 K.

Resistivity measurements confirm those obtained by DSC. However, for the samples homogenized for 30 min at 923 K (Fig. 2c), martensitic transformation was completed at the end of the thermal cycle applied (243 K). Aging treatment (24 h to 673 K) with or without stress leads to the emergence of the R-phase. This R-phase is characterized by an abrupt increase in resistivity during cooling, whereas martensitic transformation ($M \rightarrow R$) is characterized by a decrease in resistivity (Fig. 2d). On heating, the resistivity curve exhibited a small peak characterizing the inverse R-phase transformation and highlights the competition of martensite and R-phase inverse transformations due to the overlapping areas of their domains of existence. The occurrence of the R-phase is due to the aging treatment close to 673 K which leads to the precipitation of particles rich in Ni (Ti_3Ni_4) [4,5,8]. These precipitates constitute preferential sites for the nucleation of variants of the R-phase, whose parameters very close to those of crystallographic precipitates Ti_3Ni_4 [5].

3.2. Study of the All-Round Memory Effect

Fig. 3 shows the results obtained in traction after heat treatment for 24 h at 673 K without stress ($\sigma_{aging} = 0$ MPa, curves in Fig. 3a and c), and with stress ($\sigma_{aging} = 95$ MPa, curves in Fig. 3b and d). In all cases, a static stress test was applied in the high temperature phase close to 380 K and a thermal cycle was carried out between 380 and 240 K for curves in Fig. 3a and b, and between 380 and 290 K for curves in Fig. 3c and d.

Between each heat cycle, the length of the sample varied according to strain (due to the elasticity of the sample) and the number of cycles (the phenomenon of education) [9–11]. In order to compare the results for each chart in Fig. 3, the curves were shifted vertically to match the strains in the austenitic phase at the beginning of cooling. In the high temperature phase (austenite), an elongation of the sample due to thermal expansion of the sample and of the test machine was observed. Zero strain was arbitrarily set as the intersection of the right curve due to thermal expansion in the high temperature phase with a vertical line (dotted line graphs) set at 244 K for curves in Fig. 3a and b and 310 K for curves in Fig. 3c and d.

In Fig. 3a (thermal treatment without stress), the classical behavior of TiNi alloys [12,13] during thermal cycling can be seen: when the sample is not subjected to stress ($\sigma_{test} = 0$) martensitic transformation does not lead to any change in shape. Application of static stress σ_{test} at 244 K leads to strain ε_m in the direction of the stress during cooling and return close to the initial shape due to the Shape Memory Effect during heating. This strain ε_m increases with the stress σ_{test} and tends to saturation above $\sigma_{test} = 100$ MPa (curve 1 in Fig. 4a).

During cooling under $\sigma_{test} \neq 0$ an initial cooling deformation near 320 K can be observed. This strain is caused by the transformation of austenite to the R-phase. A second higher strain between 310 and 260 K is associated with the transformation of the R-phase to the martensitic phase. The temperatures of this latter transformation are much more sensitive to stress (3 MPa/K for cooling and 6 MPa/K for heating) than the austenite/R-phase transformation (20 MPa/K for cooling and 22 MPa/K for heating).

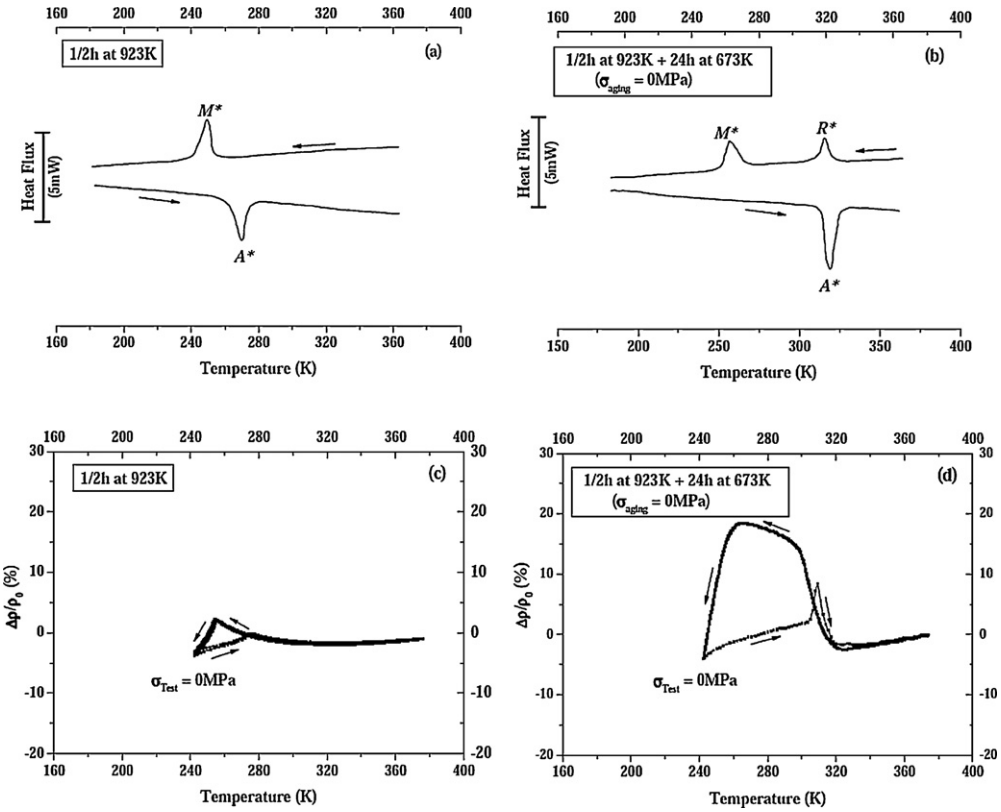

Fig. 2. DSC (a, b) and resistivity (c, d) measurements after different thermomechanical treatments.

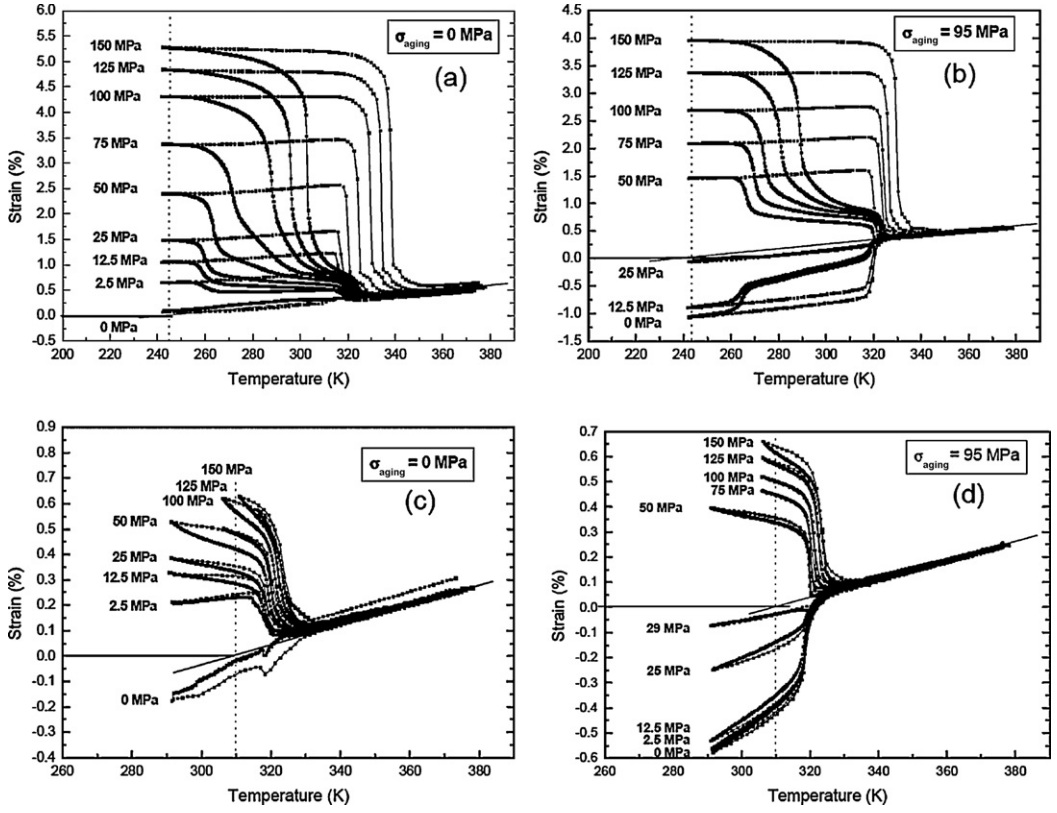

Fig. 3. Thermal cycles under variable σ_{test} stresses after thermal treatment for 24 h at 673 K without stress (a, c) and under σ_{aging} static stress of 95 MPa (b, d).

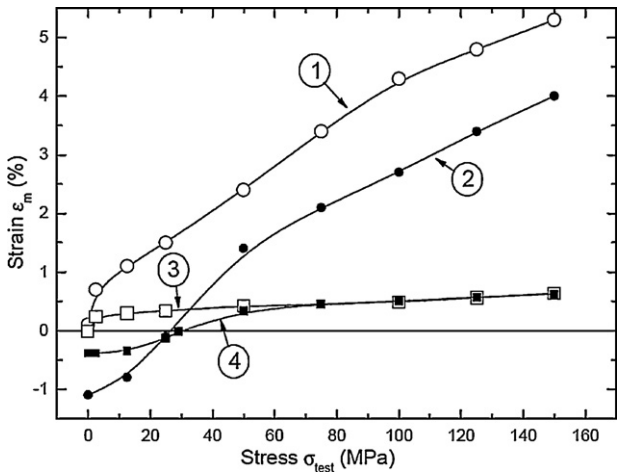

Fig. 4. ε_m versus σ_{test} stress for sample aged without σ_{aging} stress (curves 1 and 3) and with σ_{aging} = 95 MPa (curves 2 and 4), and for complete thermal cycles (curves 1 and 2) and *R*-phase transformation cycle (curves 3 and 4).

When the sample is aged under stress (σ_{aging} = 95 MPa, Fig. 2b), the zero stress cycle (σ_{test} = 0) exhibits the All Round Memory Effect: under this effect the sample spontaneously deforms on cooling in the direction opposite the stress imposed during aging. On heating, the sample recovers its initial shape by Shape Memory Effect. The sample therefore contracts during cooling and elongates during heating [14]. On cooling, the first contraction corresponds to the austenite to *R*-phase transformation, and the second contraction corresponds to the *R*-phase to martensite transformation. On heating, only the reverse martensitic martensite to austenite transformation is observed. Application of static σ_{test} stress opposite the ARME eliminates this effect for σ_{test} = 25 MPa. Stresses above 25 MPa lead to cooling deformation in the direction of the σ_{test} stress. Fig. 4 shows strain ε_m measured at 243 K for the sample annealed at 673 K both without stress (curve 1) and under stress σ_{aging} = 95 MPa (curve 2). We can see that curve 2 is shifted to the left by about 25–30 MPa when annealing at 673 K takes place under stress. This occurs since the direction of the σ_{test} stress is contrary to that of the internal stresses due to the Ti_3Ni_4 precipitates oriented by the σ_{aging} stress. The magnitude of these internal stresses caused by the precipitates can be estimated approximately at 25 MPa.

To study only the effect of the austenite to *R*-phase transformation, thermal cycles with cooling limited to 290 K (Fig. 3c and d) were performed. The amplitude of deformations and transformation hysteresis are much smaller than for martensitic transformation. The transformation temperatures also exhibit very weak dependence on stress.

For the *R*-phase transformation, the same phenomena as for complete thermal cycles were observed. The stress σ_{test} necessary to cancel the effect of the internal stresses caused by the precipitates is slightly higher but in the same order of magnitude as for the full thermal cycles (σ_{test} = 30 MPa).

Curves 3 and 4 of Fig. 4 show the ε_m strain caused by the austenite to *R*-phase transformation and measured at 310 K versus the σ_{test} stress. For the *R*-phase transformation, the strain ε_m dependence with σ_{test} is lower than for martensitic transformation, but, as for curves 1 and 2, a horizontal shift of approximately 25 MPa can be observed between curves 3 and 4.

4. Conclusion

The ARME effect is generally studied after subjecting the samples to bending stresses during aging. In this paper, we imposed this effect with tensile stresses. Preferential orientation of the precipitates Ti_3Ni_4 followed that generated internal stresses leading to the contraction of the samples during cooling.

This allowed us to quantify ARME more easily. Our results show that tensile stress in the region of 25–30 MPa applied in opposition to ARME cancels the effect of internal stresses generated by the precipitates. This gives us an order of magnitude of the amplitude of these constraints.

We measured ARME during complete thermal cycles (transformation of austenite to *R*-phase and *R*-phase to martensite), and during thermal cycling only involving the austenite to *R*-phase transformation. In both cases, the stress required to remove the effect of internal stress is of the same order of magnitude.

The curves showing the strain at low temperature versus the stress σ_{test} applied for samples aged under stress have the same shape as the curves of the sample aged without stress, but are horizontally shifted by 25 MPa. This value corresponds to the magnitude of the internal stresses due to the oriented Ti_3Ni_s precipitates.

Acknowledgement

The authors would like to thank the Franco-Algerian Huber Curien Partnership TASSILI for its financial support.

References

[1] J. Frenzel, E.P. George, A. Dlouhy, C. Somsen, M.F.X. Wagner, G. Eggeli, Acta Materialia 58 (2010) 3444–3458.
[2] J. Li, Z. Zheng, X. Li, Z. Peng, Materials and Design 30 (2009) 314–318.
[3] S. Chouf, M. Morin, S. Belkahla, G. Guenin, Materials Science and Engineering A 438–440 (2006) 671–674.
[4] M. Nishida, T. Honma, Scripta Metallurgica 18 (1984) 1293–1298.
[5] T. Honma, Proceedings of the International Conference on Martensistic Transformation (1986) 709–716.
[6] M. Sato, A. Ishida, S. Miyazaki, Thin Solid Films 315 (1998) 305–309.
[7] A. Gyobu, Y. Kawamura, H. Horikawa, T. Saburi, Materials Science and Engineering A 273–275 (1999) 749–753.
[8] T. Fukuda, M. Takahata, T. Kakeshita, T. Saburi, Materials Transactions 42 (2001) 323–328.
[9] K. Wada, Yong Liu, Materials Science and Engineering A 481–482 (2008) 166–169.
[10] C. Urbina, S. De la Flor, F. Ferrando, Journal of Alloys and Compounds 490 (2010) 499–507.
[11] S. Colombo, C. Cannizzo, F. Gariboldi, G. Airoldi, Journal of Alloys and Compounds 422 (2006) 313–320.
[12] S. Miyazaki, A. Ishida, Materials Science and Engineering A 273–275 (1999) 106–133.
[13] P. Filip, K. Mazanec, Scripta Materialia 35 (3) (1996) 349–354.
[14] T. Fukuda, A. Deguchi, T. Kakeshita, T. Saburi, Materials Transactions JIM 38 (6) (1997) 514–520.